# Modeling and Event Based Simulation of an Earthmoving Digger Using SolidWorks Premium 2014®.

**B.C. Chukwudi, Ph.D.[1*]; H.E. Opara, Ph.D.[2]; and M.B. Ogunedo, B.Eng,[1]**

[1]Department of Mechanical Engineering, Imo State University, PMB 2000, Owerri, Nigeria.
[2]Department of Civil Engineering, Imo State University, Owerri, Nigeria.

E-mail: benkeke07@yahoo.com*

## ABSTRACT

This paper presents an overview of the process involved in modeling a feasible and operational CAD model of an earthmoving digger using SolidWorks premium 2014. Concurrently, it details the procedure and results of an Event Based Simulation conducted on the CAD model. The goal of this work is to prototype the earthmoving digger before production, to study the various interactions between its components, and to finally study its event dependent behavior involved in moving a load. Graphic representations of the model are presented in this paper alongside calculations and results pertaining to the event-based motion simulation on SolidWorks®.

The model showed that changes in parameters such as digging time or trajectory influence the performance of hydraulic excavators. A shortened digging time increases the power required for the excavation process. The simulation on the effect of different digging trajectories also shows that a shallow trajectory consumes less power than a deep trajectory when the two trajectories are traveled within the same time duration. The peak power required decreases about 50% when the shallow digging trajectory is executed instead of the deep one. This paper indicates energy savings if proposed technology would be applied.

(Keywords: earthmoving digger, SolidWorks, event based motion, simulation, Newton-Euler, Kane, CAD, computer aided design)

## INTRODUCTION

Earthmovings are engineering works created through the moving or processing of parts of the earth's surface involving quantities of soil or unformed rock. The earth may be moved to another location and formed into a desired shape for a purpose. Modern earthmoving is carried out using earthmoving diggers – which are heavy construction equipment consisting of a boom, stick (ram and ram-body), bucket and cab on a rotating platform. The cab sits atop an undercarriage with tracks. All movements of the digger are accomplished through the use of hydraulic fluid, with hydraulic cylinders and hydraulic motors (Mehta, 2008).

Due to the cost and complexity involved in designing such large machines as the earthmoving digger, it is necessary to establish a medium by which the quality, efficiency and real-world applicability of such machines as can be estimated before production. Doing this would help the manufacturer with design validation, redesigning and essentially save time and cost of production. One such significantly applicable medium is virtual modeling and simulation on CAD software. Modeling helps validate and visualize the physical representation of the machine while simulation helps demonstrate how this machine will behave in a real life situation.

The purpose of this work is to create a CAD model of a feasible and operational earthmoving digger, and then with this model simulate the machine's real life behavior before production. In addition, we will study event dependent behavior of the model, attempt to understand the interactions among all its mechanical elements, and finally estimate the overall operational time of the machine. As an added benefit, we hope that this work goes a long way towards demonstrating that simulations are a very viable and applicable option within the Nigerian engineering design ecosystem.

## METHODOLOGY

The process begins with the acquisition and installation of the SolidWorks® CAD software. With this software, each part of the machine can be independently recreated, and then assembled to form the full model of the earthmoving digger.

For the Event Based motion simulation, the sequential movement of the system is first reproduced by specifying the exact time when each action occurs, as well as durations. Key frames are then specified for the adjustment of inputs or structure of mechanisms. Following this, a simulation is created where actions are triggered by events rather than time, and servomotors are used to control the actions of individual elements of the model. Finally a Gantt chart is generated to discuss the results.

### Modeling

Each component of the machine was modeled in SolidWorks using geometries that aggregate to a complete representation of the component. The major functional components for this machine are the bucket, the arm, the boom, and the ram.
Bucket: A compartment that collects materials, soil, or rubbish and dumps them to the required position.


**Figure 1:** SolidWorks Start Up Environment.

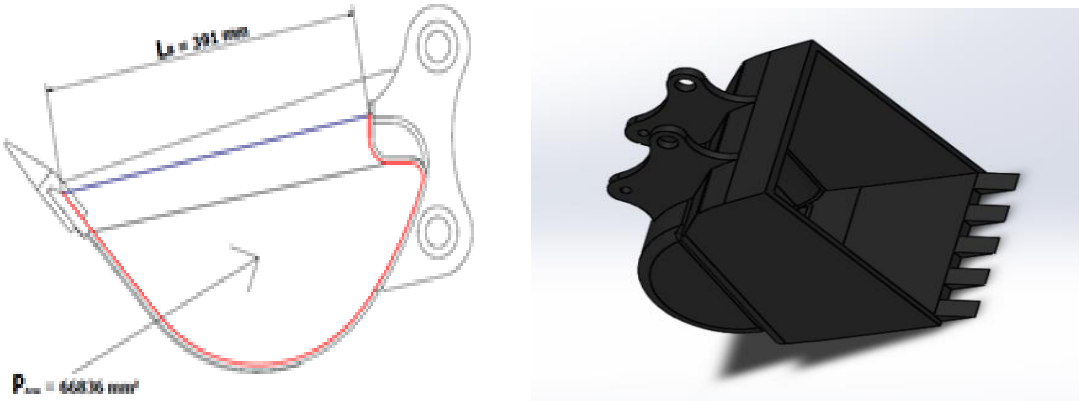

**Figure 2**: Dimensioned Earth Digger Bucket (left) and Bucket Generated in SolidWorks (right).

The bucket capacity, which is the maximum volume of material that the bucket can accommodate, was measured to be $0.028m^3$. Using this value, and an estimated soil density of $1300Kg/m^3$, the total load acting on the bucket was found to be 568.62N.

**Arm and Boom:** The arm is a solid link connecting the bucket and the boom. The boom serves as the muscle that does the lifting and the lowering of the Arm, the Bucket and the Rubbish.

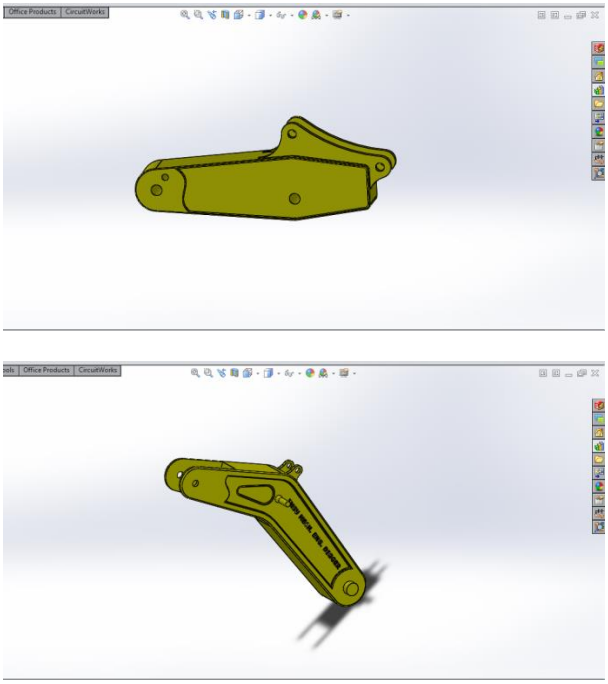

**Figure 3:** SolidWorks Part Models of Arm (above) and Boom (below).

**Rams:** A Ram is a solid cylindrical device that is displaced by fluid pressure to generate linear motion in the machine's links.

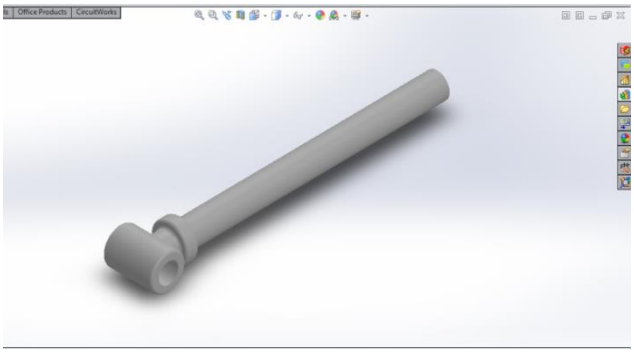

**Figure 4**: Earthdigger Ram.

Other parts were modeled in addition to the parts listed above. The ram body houses the ram and the hydraulics. The engine, counter-weight and cab form the main body of the earthmoving digger, while the track, frame and shoe form its lowest part and are responsible for the machine's translational motion.

After creation, all of these part models were then agglomerated into sub-assemblies, and eventually a final assembly of the full earthmoving digger machine. This final model is shown in the Figure 5.

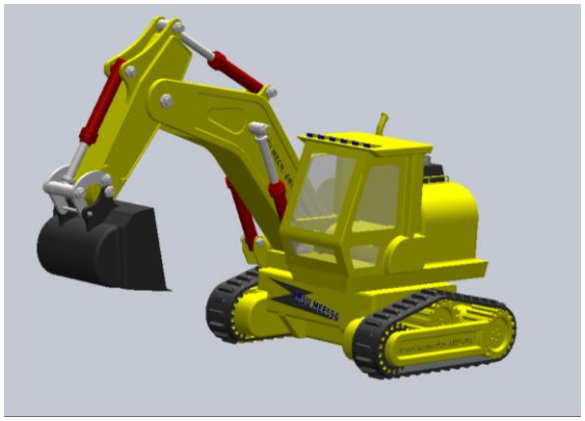

**Figure 5**: Final Assembly of Earthmoving Digger.

## Idealized Excavator Bucket

To avoid extra complexity of bucket-soil interaction in mathematical modeling, it is necessary to simplify the shape of a typical bucket. The steps in transforming an excavator bucket into an idealized bucket is based on the assumption that an excavator bucket relies on its penetration and primary and secondary separation forces for breaking soil. Therefore, the idealized bucket should have parts generating these forces. These parts include the teeth, the bottom plate, side plates and convex plate.

Firstly, the bucket teeth function as soil breaking parts by penetrating the media. The shape of the tooth usually resemble saw-edge form because its tapered cross-section facilitates a penetration process by providing proper pressures continuously to push itself into the soil media. Therefore, the shape approximation must preserve this characteristic to be reasonable replacement. In this regard, the wedge-shaped

bucket is well approximated by a cone-shaped tooth as shown in Figure 7

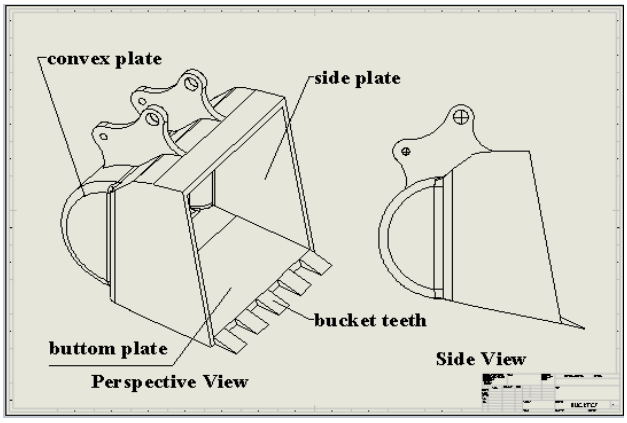


**Figure 6:** Typical Bucket: (a) Perspective view and (b) Side view

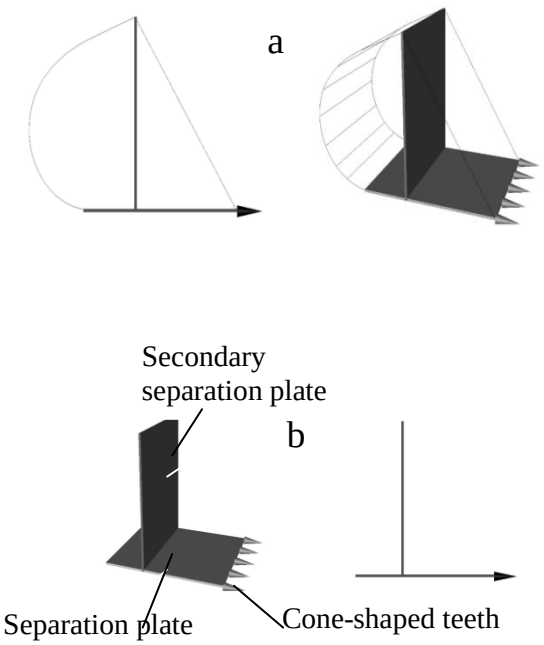


**Figure 7:** (a) Bucket Overlapped with Idealized Part (b) Idealized Bucket.

These idealized bucket parts are as summed to be equivalent to their original counter parts in terms of generating penetration, separation and secondary separation resisting forces.

## Simulation of Earth Digger Model

Figure 8 shows the structure of the simulation model. The model consists of a body sub model for reproducing the motion of earthmoving digger, and a hydraulic circuit model for reproducing the behaviors of hydraulic circuit. Actuator force is transmitted from the hydraulic circuit to the body, while actuator speed and length of the body are fed back to the hydraulic circuit.

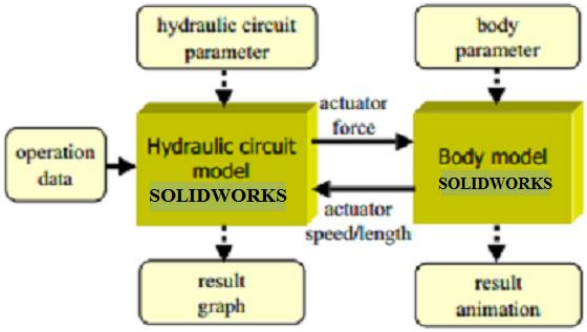


**Figure 8:** The Flowchart of the Modeling and Simulation Process.

Secondly, the bottom plate is mainly used to provide forces by which soil body contacting above it can be separated and displaced to a failure state (Note that this bottom plate is also involved in part in a penetration process by being a source of friction force with soil). Therefore, this functional characteristic is easily fulfilled by replacing the plate with a rectangular shaped plate as shown in Figure 7. This plate is referred to as a *separation plate* due to its functional role in breaking soil.

Lastly, the convex plate and the two side plates mainly contribute to the reason the ripped soil gets filled and packed in the bucket and eventually forms some kind of imaginary plane by which the soil in front of it experiences additional separation failure. Therefore, another rectangular plate, forming an ormélange with the separation plate, is the idealized part used to account for this lapsed separation mechanism as shown in Figure 7. This plate is termed the secondary separation plate.

## Mathematical Modeling of the Digger

The free body diagrams below show the velocities, moments and forces on major components of the earthmoving digger during excavation.

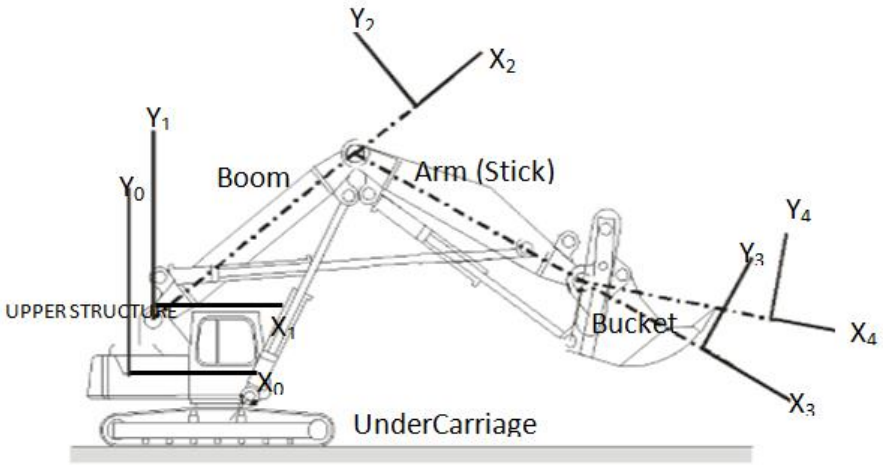


**Figure 9:** Parts of the Earthmoving Digger under Consideration and their Coordinates.

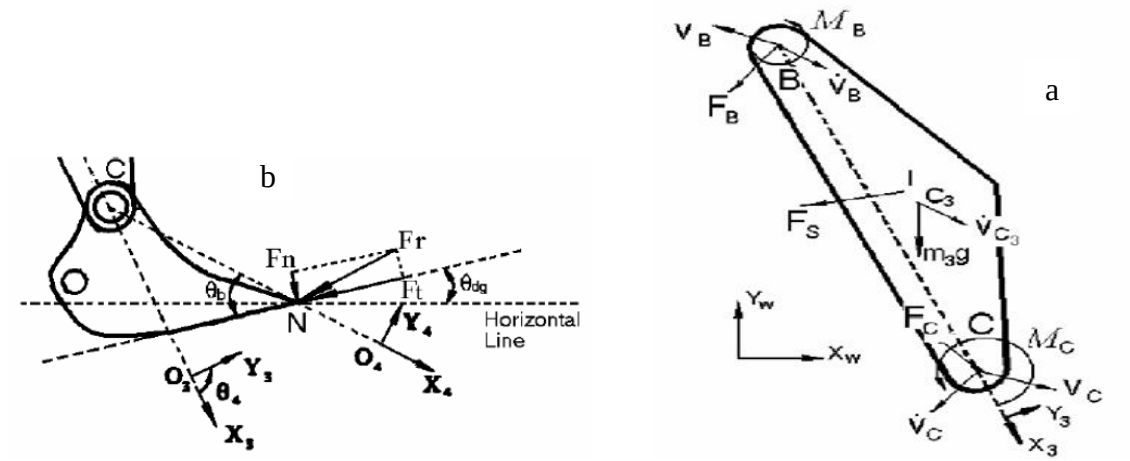


**Figure 10:** (a) The Stick (Arm) and its Coordinates, Velocity, Moments and Force, (b) The Bucket and its Coordinates and Forces.

## Newton-Euler Method

The Newton-Euler method was employed to describe the kinematics and dynamics involved in the operation of the earthmoving digger.

The velocities and accelerations are first computed iteratively for each link from boom to stick and then to bucket based on the kinematics of rigid bodies. From Figure 4, the kinematics equation for the stick are given as (Craig, 1986).

$$\vec{\omega}_{c,} = \vec{\omega}_{B,} + (\dot{\theta}_3 \vec{k})$$
$$\vec{\dot{\omega}}_{c,} = \vec{\dot{\omega}}_{B,} + (\ddot{\theta}_3 \vec{k}) + \vec{\omega}_{B,} + (\dot{\theta}_3 \vec{k})$$
$$\vec{V}_{c,} = \vec{V}_{B,} + (\dot{\theta}_3 \vec{k})\mathrm{x}\, \overrightarrow{rBC}$$
$$\vec{V}_{c,} = \vec{V}_{B,} \vec{\dot{\omega}}_{c,} \vec{r}_{BC,} + \vec{\omega}_{B,} \mathrm{x} (\vec{\dot{\omega}}_{B,} \mathrm{x} \overrightarrow{rBC})$$

Where: $\vec{\omega}_{B,}$ $\dot{\vec{\omega}}_{B}$, $\vec{\omega}_{C}$ and $\dot{\vec{\omega}}_{c}$ are the angular velocity and angular acceleration of the previous link the boom and stick, respectively. $\vec{V_B}$, $\vec{V_B}$, $\vec{V_C}$ *and* $\vec{v_C}$ are the translational velocity and translational acceleration at joint point B and C of the boom and stick, respectively. $\dot{\theta}_3$ and $\ddot{\theta}_3$ are the angular velocity and angular acceleration of the local coordinate system of the stick relative to that of the boom.

These equations can then be resolved by applying the Newton-Euler's equations to obtain the inertial forces and moments acting on the stick. Similar force equations can be generated and resolved for the boom and bucket as well.

**Kane Method**

Kane method was used to develop and analyze the structure of the static and dynamic problems associated with the hydraulic excavator. The process begins with defining the general speeds ... $u_n$ first; then the forces acting on the system are calculated, including external forces $(F_i)$ j* torques $(T_i)$j, inertia forces $(F_i)$j and inertia torques $(T_i)j^*$. Then, the motion equations are formulated as in (Fu, Gonzalez & Lee 1987):

$F_r + F_r^* = 0$

where:

$$F_r^* = \sum_{in=1}^{\infty}[(F_i)\,\mathrm{r}\frac{avi}{\sigma ur} + (T_i^*)\mathrm{r}\frac{awi}{\sigma ur}] \quad \ldots\ldots..1$$

$$F_i^* = -m_i a_i, T_i = I_i \epsilon_i \; F_i = \sum_{i=1}^{m}[(F_i)\mathrm{r}\frac{\partial \mathrm{vi}}{\sigma ur} + (T_i)\mathrm{r}\frac{\partial wi}{\sigma ur}] \quad .....2$$

The general speeds are given as: $u_1$, $u_2$, $u_3$;, where $u_1 = \theta_1, u_2 = \theta_2\; u_3 = \theta_3.$ Where the $l_1\; l_2\; l_3$ are the length of boom, stick and bucket; $\theta_1, \theta_2, \theta_3,$ are the angles of boom, stick and bucket respectively Then we can solve the partial velocity for different velocities. For example, for the points in the bucket, the partial velocities are shown as follows:

$$\frac{\partial v_1}{\partial \dot{\theta}_1} = \begin{matrix} -\sin\theta_{123} - \cos\theta_{123} \\ \cos\theta_{123} - \sin\theta_{123} \end{matrix} \begin{Bmatrix} X \\ Y \\ 0 \\ 1 \end{Bmatrix} \begin{matrix} -\sin\theta_{12} - \cos\theta_{12} \\ \cos\theta_{12} - \sin\theta_{12} \end{matrix} \begin{Bmatrix} l_2 \\ 0 \end{Bmatrix} \quad \ldots\ldots\ldots..3$$

$$\begin{matrix} -\sin\theta_1 - \cos\theta_1 \\ \cos\theta_1 - \sin\theta_1 \end{matrix}$$

$$c_1 2 = (h_{1x}\cos\theta_1 - h_{1y}\sin\theta_1 - h_{ox})^2 + (h_{1x}\sin\theta_1 - h_{1y}\cos\theta_1 - h_{oy})^2 \quad \ldots\ldots\ldots\ldots\ldots\ldots 4$$

$$c_2 2 = (l_1 + h_{21x}\, c_2 - h_{1y} s_2\, \theta_1 - h_{12})^2 + (h_{21}\sin\theta_2 - h_{21y}\cos\theta_2 - h_{12y})^2 \quad \ldots\ldots\ldots\ldots\ldots\ldots 5$$

$$c_3 2 = (l_1 + l_1 c_2 + h_{31x} c_{23} - h_{31y} s_{23} - h_{13})^2 \quad \ldots\ldots\ldots\ldots\ldots\ldots\ldots\ldots 6$$

$c_i$ is the length of boom cylinder, $c_2$ is the length of stick cylinder, $c_3$ is the length of bucket cylinder; $h_{0x}$ and $h_{0y}$, the coordinates value of a point on boom cylinder in undercarriage; $h_{1x}$ and $h_{1y}$ the coordinate value of point of boom cylinder in undercarriage; $h_{21x}$ and $h_{21y}$, the coordinate value of a point on stick cylinder in stick; $h_{12x}$, and $h_{12yx}$, the coordinate value of a point of stick cylinder in boom; $h_{31x}$, and $h_{31y}$, the coordinate value of a point of bucket cylinder in bucket; $h_{13x}$ and $h_{13y}$, the coordinate value of a point of bucket cylinder in boom.

Differentiating equation *{4, 5 and 6*), the relationship between the velocities of cylinder and linkage angle can be obtained as shown below:

$$\frac{\partial c_1}{\partial \theta_1} = \frac{1}{c_1} [h_{ox} (h_{1x} + s_1 + h_{1y} c_1 - h_{1x} c_1 + h_{1y} s_1)]$$
$$\frac{\partial c_2}{\partial \theta_2} = \frac{1}{c_2} [(l_{1x} + h_{12x}) (h_{12x} s_2 - h_{21y} c_2 - h_{21y} s_2)]$$
$$\frac{\partial c_2}{\partial \theta_2} = \frac{1}{c_3} [(l_1 + h_{13x}) (-l_2 s_2 - h_{31x} s_{23} - h_{31y} c_{23}) + (-h_{13y}) (l_2] c_2 + h_{31x} c_{23} - h_{31y} s_{23})]$$

$$T_1 \frac{\partial c_1}{\partial \theta_1} + \underset{F}{\rightarrow} \frac{\theta s_1}{\partial \theta_2} + M_3 g (x_{1 cos} \theta_1 - y_{1 \sin \theta_1}) + M_{2\,g} (l_{1 \cos \theta_1})$$
$$+ x_2 \cos \theta_{12} - y_2 \sin \theta_{12}) + M_{3\,g} (l_1 cos \theta_1 + l_1 cos \theta_{12} + x_{3 \cos \theta_{123}} - y_{23 \sin} \theta_{123}) = 0$$
$$T_2 (\frac{\partial c_2}{\partial \theta_2} + T_3 (\frac{\partial c_3}{\partial \theta_3} + \underset{F}{\rightarrow} \frac{\vec{\theta s_1}}{\partial \theta_2} + M_{2\,g} (x_{2 \cos \theta_{12}} - y_{2 \sin} \theta_{12})$$
$$+ M_{3\,g} (l_2 cos \theta_{12} + x_3 cos \theta_{123} - y_{3 \sin} \theta_{123}) = 0$$
$$T_3 (\frac{\partial c_3}{\partial \theta_3} + \underset{F}{\rightarrow} \frac{\vec{\theta s}}{\partial \theta_3} + M_{2\,g} (x_{3 \cos \theta_{12}} 3 - y_{2 \sin} \theta_{123}) = 0$$

According to the static equations, some physical significance of items can be studied. The three equations are corresponding to three general speed $u_1, u_2$ and $u_3$.

Therefore, $T_1 \frac{\partial c_1}{\partial \theta_1}$ ; $T_2 \frac{\partial c_2}{\partial \theta_2}$ + $T_3 \frac{\partial c_3}{\partial \theta_3}$ and $T_3$ - are the driving torques to $\theta_1, \theta_2, and\ \theta_3$.
For torque $T_1 \frac{\partial c_1}{\partial \theta_1}$, $\frac{\partial c_1}{\partial \theta_1}$ is the arm force.

Similarly, the components on whole system can be analyzed.

## RESULTS

### Simulation

Three different initial conditions are considered to start and run the simulator:

***a. Force Conditions:*** The hydraulic force inputs to the cylinders and the digging force to the tip of the bucket are applied and the time response of the system is then obtained by measuring the displacement, velocity and acceleration of each joint and the extension displacement, extension velocity and extension acceleration of each cylinder.

***b. Displacement Condition:*** A digging trajectory at the bucket tip is prescribed as input. The model solves for the required displacement input for each cylinder to achieve that trajectory. It also output other parameters such as joint angles, angular velocity and acceleration.

***c. Mixed condition:*** The extension displacement of each cylinder combined with a prescribed resistive force at the bucket tip is prescribed as the input. With the time dependence of the extension displacement of each cylinder and the resistive force known, the hydraulic force inside

each cylinder and joint force between two links can be evaluated.

**d. Other assumptions are:**

(i) There is no joint friction between the upper structure and the assembly and between the links within the assembly; and

(ii) the hydraulic cylinders are ideal, i.e., no frictional losses Figure 17 shows a hydraulic excavator simulator developed in SolidWorks 2014 Premium motion environment. Figure 5 shows 3D solid hydraulic excavator model, while Figure 19 shows a virtual prototype. Only the front-end assembly including boom, stick and bucket of the hydraulic excavator is modeled for the reason described in the previous section.

## DATA PRESENTATION AND DISCUSSION

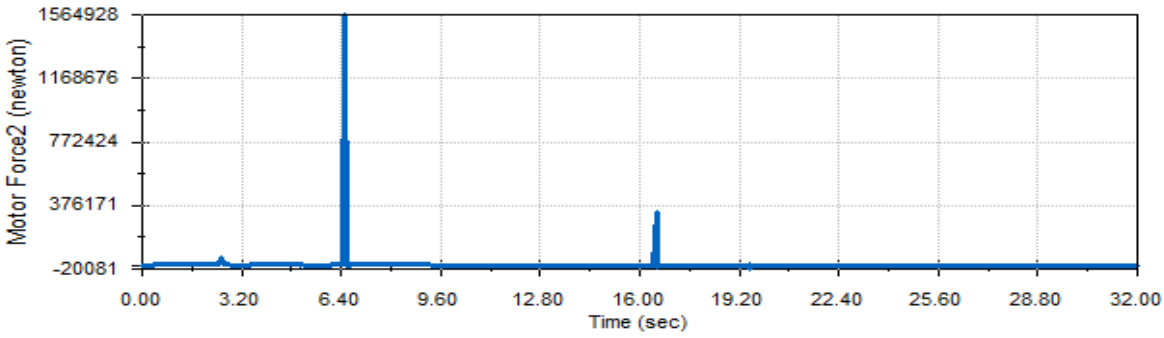


**Figure 11**: Variation of Boom Motor Force (N) with Time (sec).

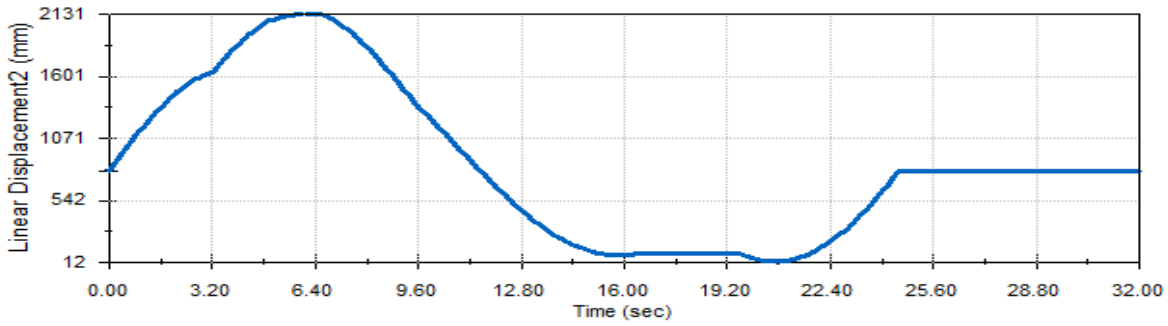


**Figure 12**: Variation of Boom Linear Displacement (mm) with Time (sec).

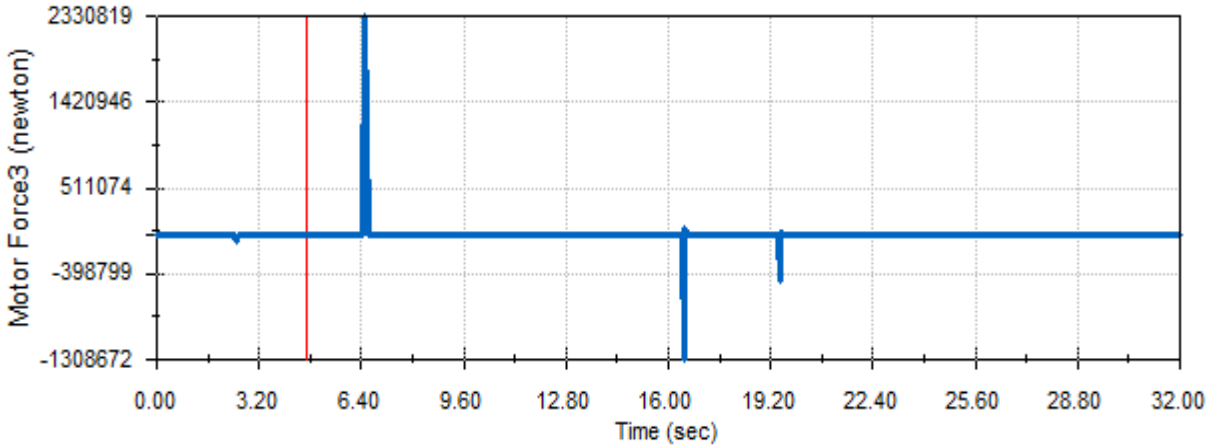


**Figure 13**: Variation of Arm Motor Force (N) with Time (sec).

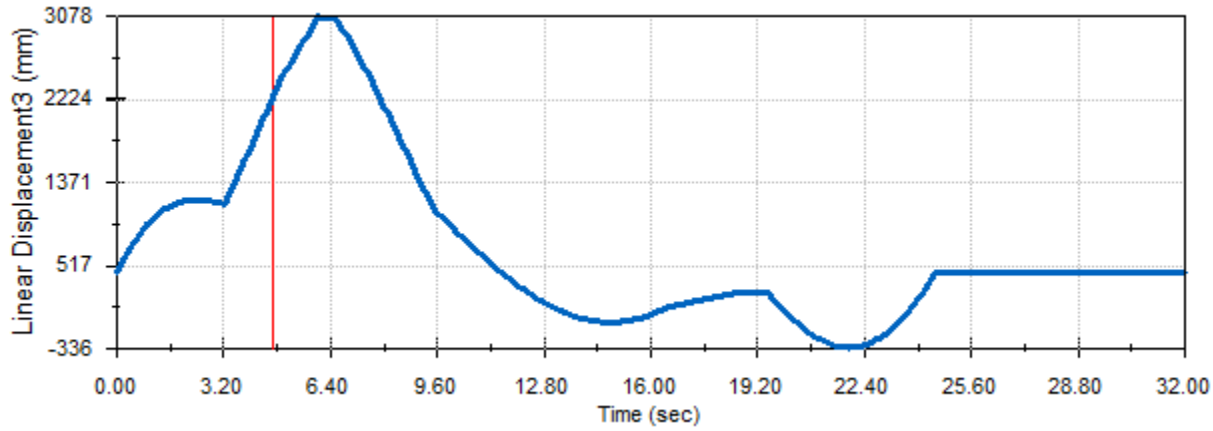


**Figure 14:** Variation of Arm Linear Displacement (mm) with Time (sec).

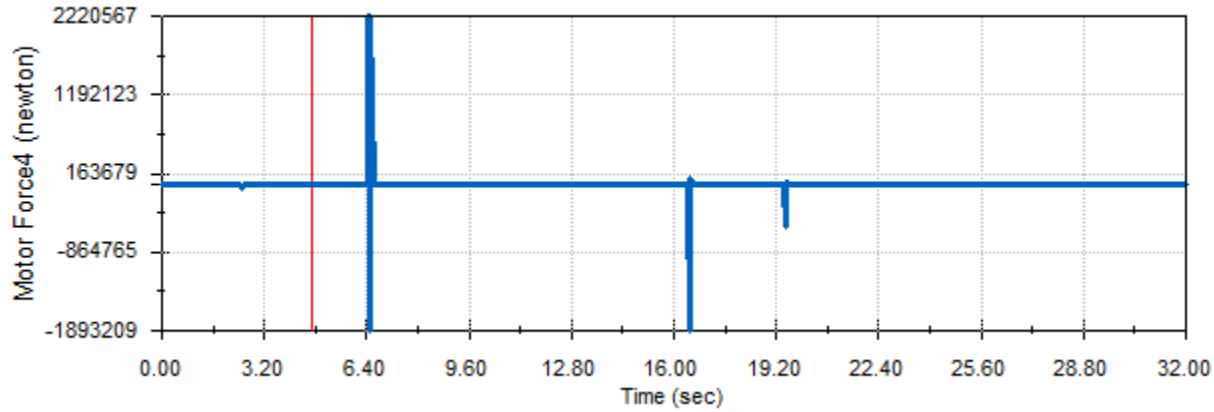


**Figure 15**: Variation of bucket motor Force (N) with time (sec)

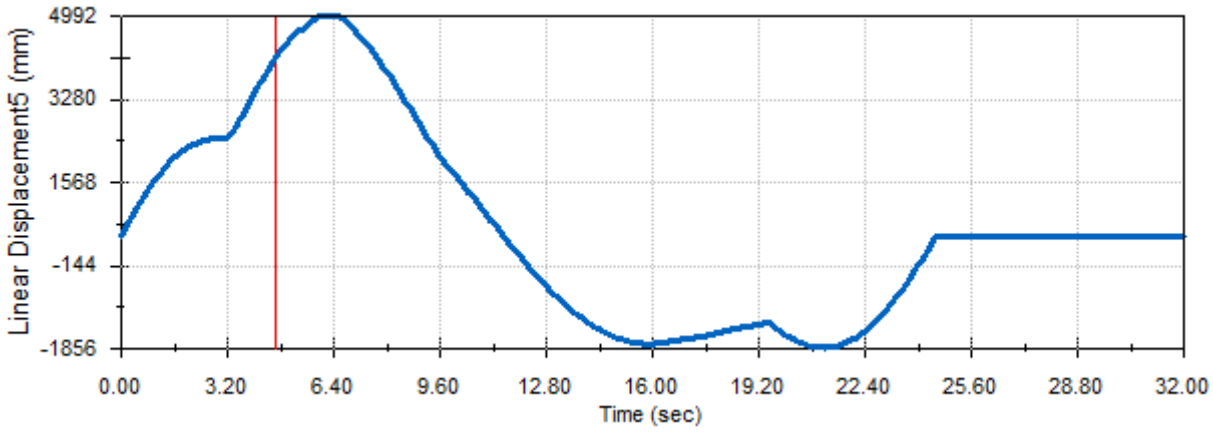


**Figure 16**: Variation of Bucket Linear Displacement (mm) with Time (sec).

Figures 11 to 16 show a single phase result of the motion of the individual components for both the acting forces and the displacements in the x-axis. The peak of each action is observed to take place in 6.4seconds of the events. In the force analysis, this shows that the digger goes against all resistance when it is freely moving, not at the beginning of the event nor at the end of the event, rather at the mid period of the event.

## Test Examples

Examples are included to illustrate the performance of hydraulic excavator based on given digging paths and to define efficient digging profiles based on energy consumption. The kinematics and dynamic simulations of hydraulic excavator are illustrated by prescribing an assumed trajectory at the bucket tip when excavating a formation or muck-pile (as illustrated in Figure 20).

The formation or muck-pile has a slope of 50 degrees. The trajectory is designed such that at the end of its execution, the volume of the cut material is equal to the bucket capacity of the excavator. The bucket tip moves at constant speed and it takes 7.5 seconds to execute the entire trajectory. The main geometry data for the excavator simulated is listed in Table 1, while the parameters for determining the resistive force are shown in Table 2.

**Table 1:** Main Hydraulic Shovel Data [Alaydi, 2008]

| Component | Length* (m) | Mass (kg) | Inertia Moments** ( Kg. $m^2$ ) |
|---|---|---|---|
| Boom | 7.682 | 36420 | 1.850E + 005 |
| Stick | 5.334 | 21310 | 4.810E + 004 |
| Bucket | 3.950 | 40800 | 4.567E + 004 |
| Bucket capacity 5.625$m^3$ | | | |

*Length between two joints for boom and stick and between joint and bucket tip for bucket
**Moment of inertia about the gravitational center

**Table 2**: Data for Excavated Material Properties [Luengo et al., 1988].

| Kp | 1.005 | Ɛ | 55.000 kg /($m^2$ / $s^2$ ) |
|---|---|---|---|
| Ks | 5.500 | | |
| μ | 0.1 | B | 4.8 m |
| N | 1 kg . $m/s^2$ | | |

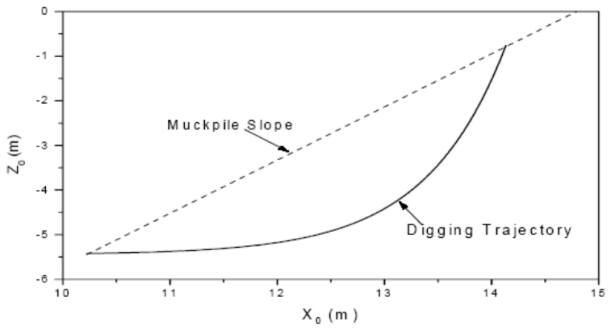


**Figure 17**: Trajectory for the Bucket Tip.

Given the geometrical and physical parameters for the excavator and the cutting material, the evolution of the joint angles and cylinder forces with time are shown in attached figures based on the given trajectory curve. It is also shown that the cylinders experience three phases during the digging part: a gradual increase, reaching maximum and gradual decrease. The force reaches its maximum around the middle of the trajectory.

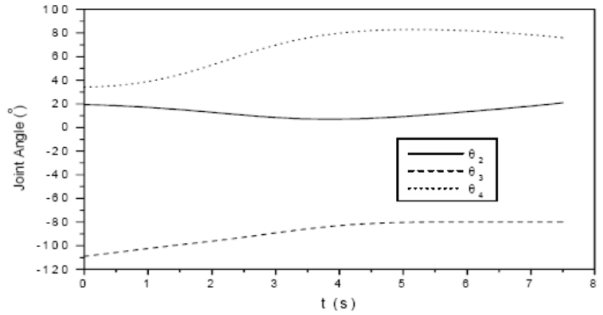


**Figure 18**: Changing Joint Angle with Time during Excavating.

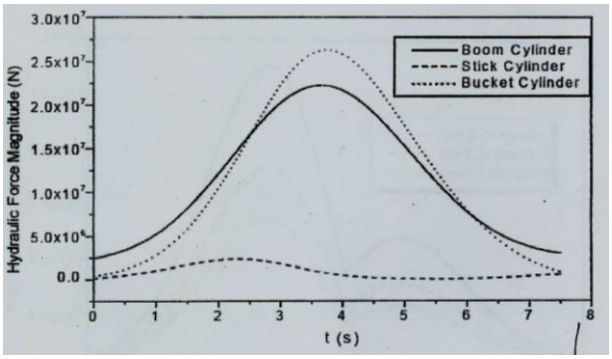


**Figure 19:** Force Changing with Time During Excavating.

It is often required in surface mining industry that the duty cycle is shortened in order to improve production efficiency. This is particularly important for large-scale operations where excavators are over-trucked. Even reducing the execution time of a single cycle of an operation by a few seconds can translate into large savings over the entire job.

The same trajectory as shown in Figure 18 is completed within three different digging times: 5, 7.5 and 10 seconds. The power consumption for the three different times are simulated as shown in Figure 20. It can be seen that shortening the digging time consumes more energy. The peak power required almost doubles when the digging time is reduced by half. Therefore, there is a need for a trade-off between energy consumption and saving duty cycle.

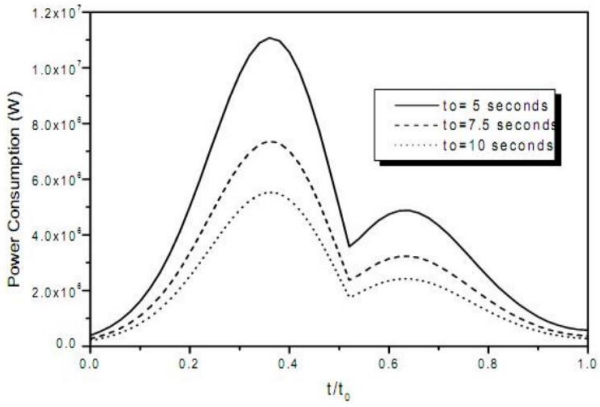


**Figure 20**: Trajectory Power Consumption for the Three Different Excavating Times.

Digging trajectory is a very important factor that influences the performance of a hydraulic excavator. Three different trajectories are considered with the end point on each trajectory being reached at the same time of 7.5 seconds and with full bucket loading capacity. The digging trajectories are shown in Figure 20.

The corresponding power consumption for the trajectories are shown in Figure 22 (case 1 corresponds to the trajectory with short but deep digging, case 3 with long but shallow digging and case 2 in between the first two cases). It can be seen that a short but deep trajectory (case 1) requires more power consumption than a long but shallow one. The peak power required decreases by 50% when the shallow digging trajectory is executed instead of the deep one.

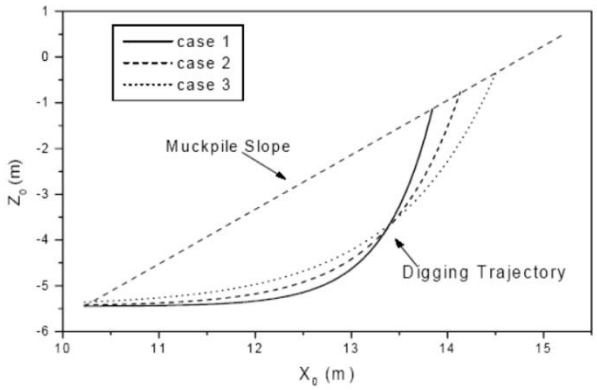


**Figure 21:** Three Trajectories for Bucket Tip of Hydraulic Excavator.

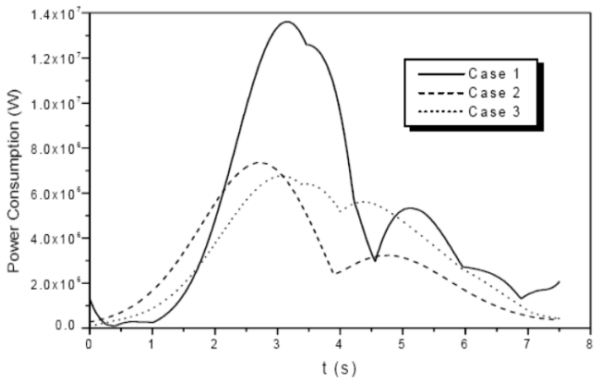


**Figure 22:** Corresponding Power Consumption for the Trajectories.

## CONCLUSION

The parameterized characteristics of the simulator make it easy to investigate digger performance under various working conditions. The simulator captures the kinematics and dynamics of the excavator within its operating environment, thus providing a powerful tool for performance monitoring, excavation process designs and the structural optimization of excavators. Simulation also enables a virtual prototyping environment for complex mechanical systems and performing detailed analysis before detailed design and/or manufacturing to minimize the use of costly physical prototypes.

Based on results of this paper, it can be concluded that changes in parameters such as digging time or trajectory influence the performance of hydraulic excavators, as indicated by different power consumptions for different digging times and different digging trajectories. A shortened digging time increases the power required for the excavation process. The peak power required almost doubles when the digging time reduces half. The simulation on the effect of different digging trajectories also shows that a shallow trajectory consumes less power than a deep trajectory when the two trajectories are traveled within the same time duration. The peak power required decreases about 50% when the shallow digging trajectory is executed instead of the deep one. This paper indicates energy savings if proposed technology would be applied.

## REFERENCES

1. Alaydi, J.Y. 2008. "Mathematical Modeling of Pump Controlled System for Hydraulic Drive Unit of Single Bucket Excavator Digging Mechanism". *Jordan Journal of Mechanical and Industrial Engineering*. 2(3):157 – 162.

2. Craig, J.J. 1986. *Introduction to Robotics: Mechanics and Control*. Addison-Wesley Publishers: New York, NY.

3. Fu, K.S., R.C. Gonzalez, and C.S. Lee. 1987. *Robotics: Control, Sensing,Vision and Intelligence*. McGraw Hill: New York, NY.

4. Luengo, O., S. Singh, and H. Cannon. 1998. "Modeling and Identification of Soil-Tool Interaction in Automated Excavation". *Proceedings of the 1998 IEEE/RSJ International Conference on Intelligent Robots and Systems*. Victoria, BC, Canada.1900-1906.

5. Mehta Gaurav, K. 2008. "Design and Development of an Excavator Attachment". M. tech Dissertation Thesis. Nirma University, Institute of Technology: Ahmadabad.

## SUGGESTED CITATION

Chukwudi, B.C., H.E. Opara, and M.B. Ogunedo. 2015. "Modeling and Event Based Simulation of an Earthmoving Digger Using SolidWorks Premium 2014". *Pacific Journal of Science and Technology*. 16(2):5-16.